2014

Ultrahigh Vacuum Cryostat System for Extended Low Temperature Space Environment Testing

Justin Dekany
Utah State University

Robert H. Johnson
Utah State University

Gregory Wilson
Utah State University

Amberly Evans Jensen
Utah State University

JR Dennison
Utah State Univesity

Recommended Citation

Justin Dekany, Robert H. Johnson, Gregory Wilson, Amberly Evans and JR Dennison, "Ultrahigh Vacuum Cryostat System for Extended Low Temperature Space Environment Testing," IEEE Trans. on Plasma Sci., 42(1), 2014, 266-271. DOI: 10.1109/TPS.2013.2290716

Ultrahigh Vacuum Cryostat System for Extended Low Temperature Space Environment Testing

Justin Dekany, Robert H. Johnson, Gregory Wilson, Amberly Evans and JR Dennison

***Abstract*— The range of temperature measurements have been significantly extended for an existing space environment simulation test chamber used in the study of electron emission, sample charging and discharge, electrostatic discharge and arcing, electron transport, and luminescence of spacecraft materials. This was accomplished by incorporating a new two-stage, closed-cycle helium cryostat which has an extended sample temperature range from <40 K to >450 K, with long-term controlled stability of <0.5 K. The system was designed to maintain compatibility with an existing ultrahigh vacuum chamber (base pressure $<10^{-7}$ Pa) that can simulate diverse space environments. These existing capabilities include controllable vacuum and ambient neutral gases conditions ($<10^{-8}$ to 10^{-1} Pa), electron fluxes (5 eV to 30 keV monoenergetic, focused, pulsed sources over 10^{-4} to 10^{10} nA-cm^{-2}), ion fluxes (<0.1 to 5 keV monoenergetic sources for inert and reactive gases with pulsing capabilities), and photon irradiation (numerous continuous and pulsed monochromated and broad band IR/VIS/UV [0.5 to 7 eV] sources). The new sample mount accommodates 1 to 4 samples of 1 cm to 2.5 cm diameter in a low temperature carousel, which allows rapid sample exchange and controlled exposure of the individual samples. Custom hemispherical grid retarding field analyzer and Faraday cup detectors, custom high speed, high sensitivity electronics, and charge neutralization capabilities used with <50 pA, <5 μs, $<3\cdot10^3$ electrons/pulse pulsed-beam sources permit high-accuracy electron emission measurements of extreme insulators with minimal charging effects. *In situ* monitoring of surface voltage, arcing, and luminescence (250 nm to 5000 nm) have recently been added.**

***Index Terms*—materials testing, electron emission, space environment, low temperature, ultrahigh vacuum, cryostat, instrumentation**

I. Introduction

To better understand the effects of the space environment on materials used in spacecraft construction it is important to test these materials under highly controlled laboratory conditions. When simulating the space environment three key conditions to consider are pressure, radiation, and temperature. A space environment simulation chamber operating at ultrahigh vacuum with electron, ion and photon flux capabilities [1] has been extended to a wider operational temperature range allowing simulation of a broader range of space environment temperatures.

Electron transport and emission properties are central in understanding, modeling and mitigating spacecraft charging concerns; they are particularly susceptible to temperature changes, often exhibiting Arrhenius behavior ~$[(1/k_BT)\exp(-E/k_BT)]$. For example one of the mechanisms for exciting electrons into the conduction band is through thermal excitation [2]. As the temperature decreases, thermally excited electrons are less prone to move through an insulating material, leading to greater likelihood for charge build up. In the case of a spacecraft which is exposed to varying amounts of electron flux densities and electron energies, this environment can cause isolated regions made primarily of insulating material to electrostatically discharge. Electrical—and in some cases mechanical—failure caused by Electrostatic Discharge (ESD) is the leading source of damage to spacecraft due to the space environment [3]. Understanding these effects by better simulating the space environment over a broader range of temperatures encountered in space is the driving force behind these chamber modifications.

II. Experimental Test Chamber Design

An existing space environment simulation chamber has been designed to allow for a wide range of electron flux and energy bombardment while maintaining ultrahigh vacuum and continuous control of sample temperature. The capabilities of the chamber are summarized first. The focus of this paper is the design of the low temperature stage and the associate sample mounting system. An example of the use of the new low temperature stage for electron-induced luminescence and arcing experiments demonstrates the versitility of the design.

A. Electron Emission Test Chamber

The electron emission test chamber uses standard mechanical and turbomolecular pumps (V; see legend in Fig. 1) for roughing and an ion pump (W) for continuous maintenance-free operation (base pressure of $<10^{-7}$ Pa). Absolute pressure is monitored with Convectron and ion gauges (X). Partial pressure is measured with a residual gas analyzer (Y).

Research was supported by funding from the NASA Goddard Space Flight Center. Justin Dekany, Robert Johnson, Greg Wilson, Amberly Evans and JR Dennison are with the Materials Physics Group in the Physics Department at Utah State University in Logan, UT 84322 USA (e-mail: jdekany.phyx@gmail.com, bj68127@yahoo.com, GregdWilson@gmail.com, amb.eva@aggiemail.usu.edu, JR.Dennison@usu.edu). Dekany, Wilson and Evans are graduate students in the USU Physics Department. Dennison is a professor in that department. Johnson is an undergraduate student in the Mechanical Engineering Department at USU.

Color versions of one or more figures in this paper are available online at http://ieeexplore.ieee.org.

Digital object identifier .

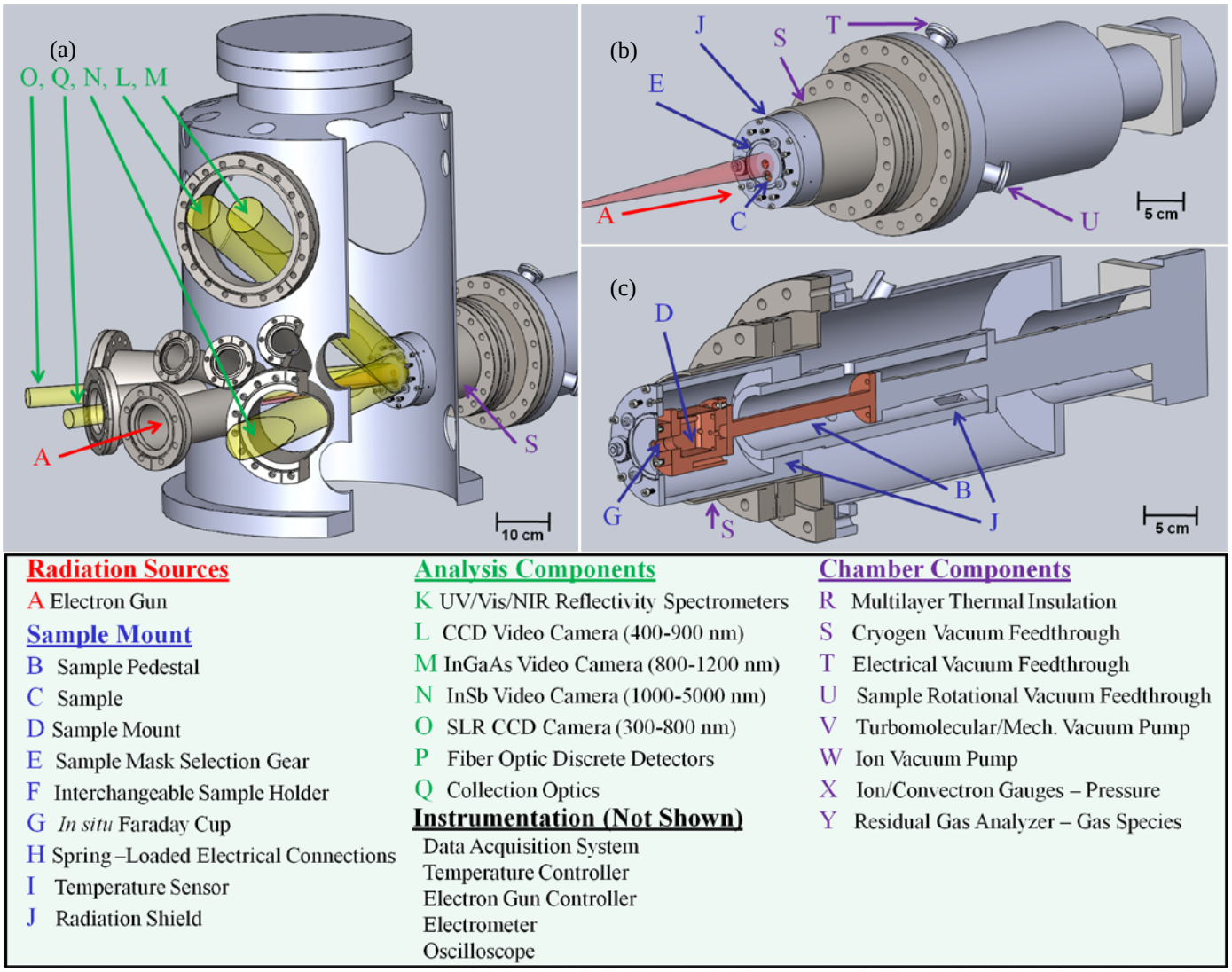

Fig. 1. Experimental test chamber. (a) Chamber exterior view with cutaway showing the various analysis component lines of sight. The electron gun is positioned on axis with the sample plane. (b) Cryostat chamber mount, showing the electron beam trajectory (red). (c) Cutaway view of cryostat showing the first stage radiation shroud and second low temperature stage with sample mount and pedestal (red).

Electron flux is produced with a high energy gun (Kimball, Model EGPS-21B)1(A), which provides a monoenergetic beam with a flux of ~1pA/cm^2 to 1 μA/cm^2 over an energy range of 5.00 to 30.00±0.01 keV. For experiments described here a continuous beam mode was used, with a broad defocused beam of ~2 cm diameter FWHM; focused, pulsed beams are also possible. The current is monitored in real-time using an *in situ* Faraday cup (G) located in the center of the sample mount (D). Currents are measured using a fast, sensitive picoammeter with <0.2 pA resolution [5]. Additional lower energy electron gun sources (5 eV to 5 keV), ion sources (100 eV to 5 keV), and photon sources (~150 nm to 2000 nm) are also available in the chamber.

Light detection uses several cameras calibrated *in situ* using NIST traceable methods, allowing for absolute spectral radiance values to be obtained. The cameras are positioned with clear views of the sample through vacuum port windows; this allows collection of photon emission data resulting from electron-induced cathodoluminescence and arcing [4]. A Single Lens Reflex (SLR) CCD camera (O) (Cannon, EOS Rebel XT DS126071; ~400 nm to 700 nm) captures 10 Mpixel visible light images at 30 s shutter speeds and full aperture with a 55 mm lens, giving it an average spectral response of ~4·10^9 counts/(W/cm^2·sr·μm). An image-intensified CCD video camera (L) (Xybion, ISG-780-U-3; ~400 nm to 900 nm) collects data at 30 frames per sec using a 55 mm lens had a spectral response of ~4·10^{10} counts/(W/cm^2·sr·μm). An InGaAs video camera (M) (Goodrich SU320MX-17RT; 800 nm to 1700 nm), is operated at ambient room temperature collecting data at 60.1 frames per second. It has a spectral response of ~1·10^9 counts/(W/cm^2·sr·μm) using a 35 mm lens. An InSb video camera (N) (Santa Barbara Focalplane SBF180), operating at liquid nitrogen temperatures, acts as a low spatial resolution mid-IR detector. The photon response of this detector increases in sensitivity with increasing wavelength ranging from 1 μm to 5.5 μm at varying integration times ranging (~10 Hz to ~30 Hz) depending on the band pass filters used; it has a spectral responsivity of ~7·10^7 counts/(W/cm^2·sr·μm).

Two fiber optics-based spectrometers (K) provide Ultraviolet/Visible/Near Infrared photon spectral measurements from ~250 nm to 1700 nm. The UV/Vis

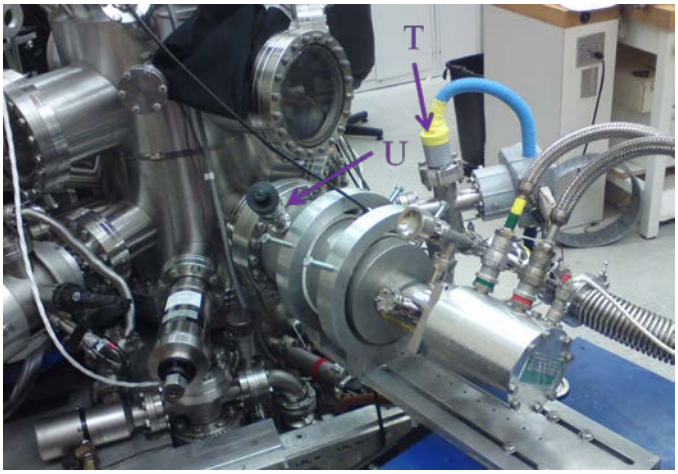

Fig. 2. Cryostat connected to the electron emission test chamber.

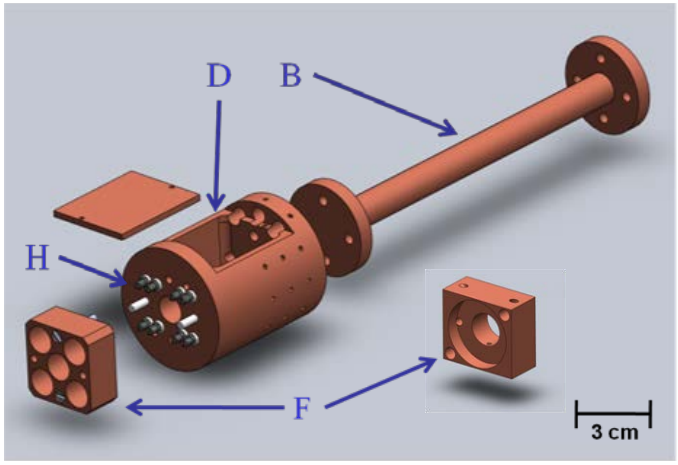

Fig. 3. View of cryostats second stage sample pedestal and interchangeable sample holder which attaches to the cryostat. Shown is a sample holder for four 1 cm diameter samples and a central Faraday cup and for a single 2.5 cm diameter sample.

spectrometer (Stellarnet, 13LK-C-SR; ~200 nm to 1080 nm) has a wavelength resolution of ~1 nm, while the NIR spectrometer (Stellarnet, RW-InGaAs-512; ~1000 nm to 1700 nm) has a ~3 nm resolution. Both detectors are housed in a piezoelectric cooler which maintains -20 K from ambient. A 4 cm diameter MgF collection optic focuses the emitted light into a 1 μm fiber optic cable routed to the spectrometers.

Although not used for the measurements described in this paper, the new cryostat/sample mount is compatible with electron detection capabilities as well. The primary detector for emission studies is a custom hemispherical grid retarding field analyzer (HGRFA), with a retarding-field analyzer grid system for emitted-electron energy discrimination between backscattered electrons (energies >50 eV) and secondary electrons (energies <50 eV). By ramping the grid bias, energy spectra of the emitted electrons can also be measured using this detector. The HGRFA features a fully-encasing hemispherical collector for full capture of emitted electrons, which is particularly well suited and calibrated for absolute yield measurements. The HGRFA can be positioned in front of a single sample mounted at the end of the cryostat.

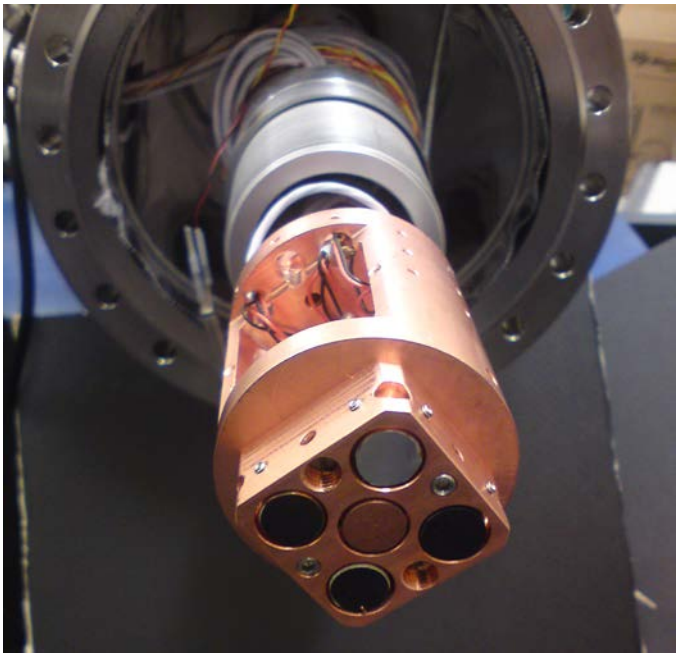

Fig. 4. Interchangeable sample holder with four 1 cm samples attached to the sample mount.

B. Low Temperature Stage Design

A closed-cycle helium cryostat has been added to the space environment simulation chamber to extend the operational temperatures for sample testing from <40 K to >450 K. Temperature is maintained to ±0.5 K using a standard computer-controlled PID temperature controller (RMC Cryosystems CR31-21) under Labview™ command and platinum RTDs (I) mounted on the sample holder, low temperature stage, and cryostat radiation shield. A large mass radiation shield (J) is attached to the cryostat's first stage (thermal load capacity of ~10 W at ~80 K) and a sample mounting stage is attached to the cryostats second stage (thermal load capacity of ~1 W at ~20 K); these large thermal masses help maintain a constant sample temperature. Due to radiative heat transfer from the chamber walls, the addition of a multilayer thermal insulation blanket (R) wrapped around the first stage radiation shield (J) is required. This blanket consists of five sheets of thin conducting material separated by a thin mesh of insulating material. With this addition to the apparatus, the sample holder which is mounted to the cryostats second stage sample pedestal (B) can reach <40 K, a temperature comparable to passively cooled spacecraft in standard orbit. Direct measurement of a sample confirmed a <2 K gradient between the samples and sample holder on which the temperature probe is mounted. Once the chamber is down to pressures of $<5\cdot10^{-3}$ Pa, the cryostat cools the sample at a rate of ~ 1 K/min, reaching the lowest temperature of ~40 K in about 4 hr; this temperature can be sustained for weeks. Heating the sample is accomplished using a combination of control and bulk heaters attached to the radiation shroud and sample mount. Once activated, the temperature controller can heat the sample at a rate of ~ 1.5 K/min and can maintain intermediate temperatures from <40 to > 450 K. Fig. 7 shows a typical cooling and heating profile.

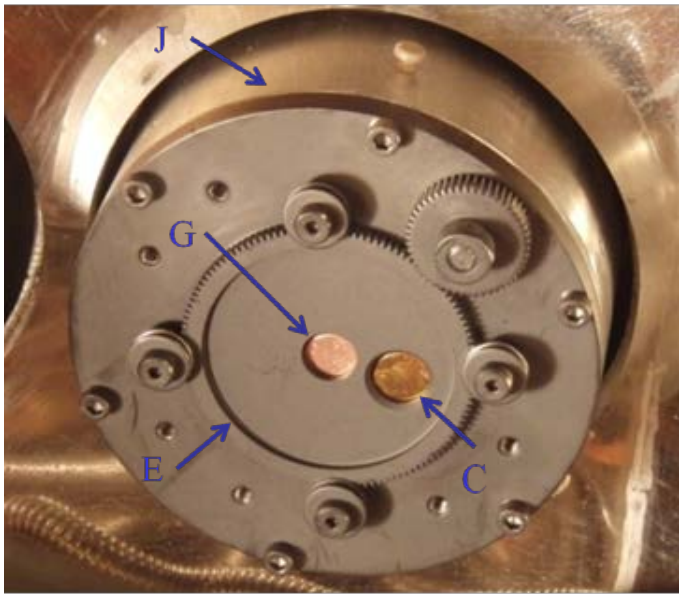

Fig. 5. Sample selection gear controlled using an external rotation translation (U). The gear/sample mask to access the Faraday cup (G) and one of four 1 cm diameter samples is shown.

The cryostat (see Fig. 1(b)) can be removed from the electron emission chamber and installed on other vacuum chambers that have an available 10 cm or 15 cm port.

C. Sample Carousel Design

The sample mount (D) has a versatile design that allows for a variety of configurations and sample sizes. Multiple sample holders (F) can be quickly interchanged with the use of spring-loaded, electrically-isolated electrode connectors (H), as shown in Fig. 3. The sample stage is electrically isolated with a Kapton spacer and PEEK screws, but maintains good thermal contact with the sample stage. The sample stage has a large wiring cavity (D) to facilitate various low-noise electrical connections, in addition to allowing room for bulk and control heaters.

In one configuration, four 1 cm diameter samples can be installed with an optional *in situ* Faraday cup (G) in the center location allowing for real-time monitoring of electron beam current (see Fig. 4). Samples in this configuration are mounted on (10.0 ± 0.1) mm diameter Cu cylinders, usually using UHV compatible, low-temperature, conductive epoxy (Masterbond, EP21TDCS-LO). The Cu cylinders are mounted in sample blocks using ceramic pins or 100 μm diameter sapphire spheres held in place with set screws to provide electrical isolation (see Fig. 4). Electrical connections to the sample are made via one or more spring loaded pins from the rear, allowing the sample current(s) to be monitored. Using this configuration, a sample mask selection gear (E) coupled to an external rotation translation feedthrough (U) allows masking of the samples not being tested (see Fig. 5); this minimizes potential sample charging of these samples. The sample mask also minimizes the amount of sample area exposed to the higher temperature chamber walls, since the mask is attached to the 80 K second stage of the cryostat. Larger samples of up to 2.5 cm by 2.5 cm square can be tested using a different sample mount (D), as shown in Fig. 6.

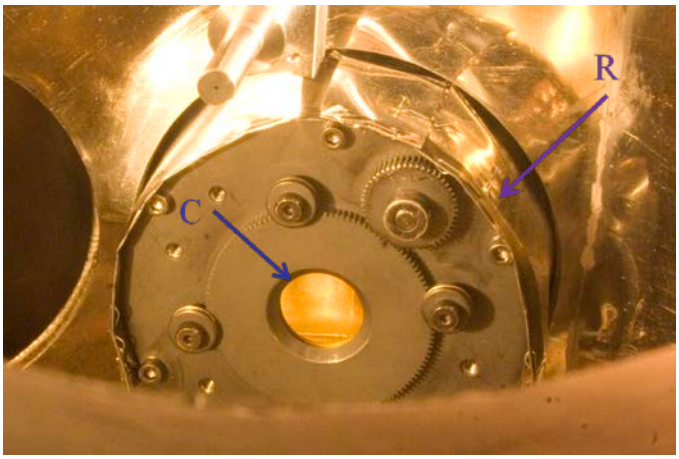

Fig. 6. Face plate with a 2.5 cm diameter sample mounted. Note radiation blanket wrapped around first stage radiation shield (J) of cryostat.

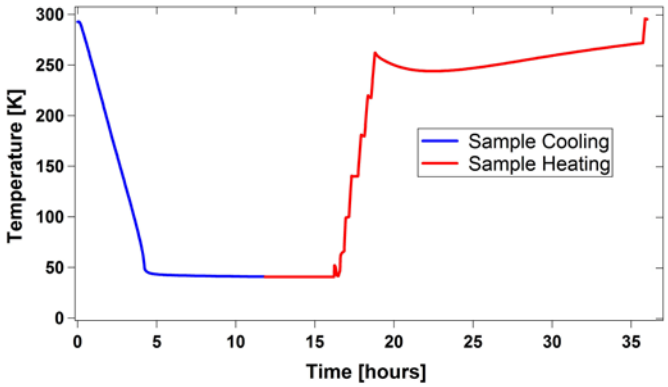

Fig. 7. Typical sample stage cooling and sample heating curves, with multiple sustained temperatures shown during heating cycle.

III. Applications

To highlight the capabilities of the low temperature cryostat incorporated into the space environment simulation test chamber, we present data from a study of the temperature dependence of electron-induced luminescence and arcing from spacecraft materials. With the various imaging detectors all focused at the sample (see Fig. 1(a)), a wide range of spectral analysis is possible [4]. Operation in a closed chamber in a dark room makes it possible to measure very low intensity sources.

An example of this is shown in still frames captured with a CCD video camera. Figure 8(a) shows a 1 cm sample, illuminated using a dim fiber optic timing light to show the region to be exposed to the electron flux. Figures 8(b) and 8(c) show a comparison of the effect temperature has on this material; the glow at 293 K is hardly detected with this imaging camera, but as the temperature is decreased to 40 K intensity increases (roughly linearly) and a prominent glow is clearly evident. If enough charge is built up in the material, arc events may occur [6] where the charge in the sample finds a conduction path to the edge of the grounded sample holder (F). The very intense optical signature of an arc was captured in a video frame shown in Fig. 8 (d). Figure 9 shows simultaneous measurements from an arc event as recorded by the electrometer and the CCD video camera. Here a constant current density of 1 nA/cm^2 was incident on the 1 cm sample

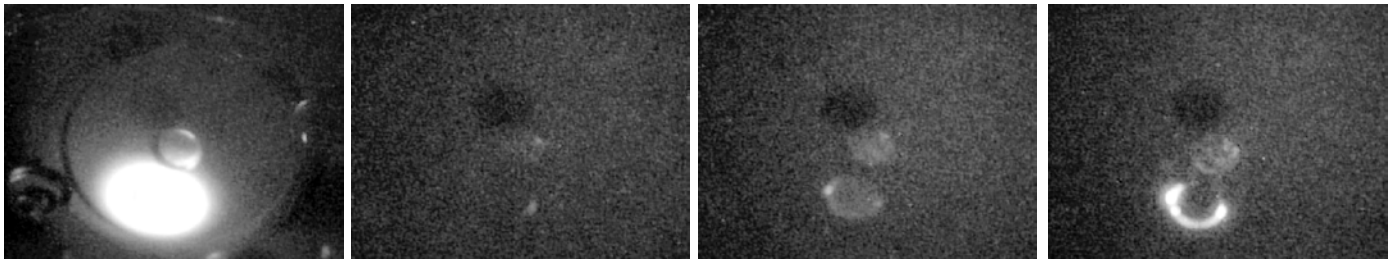

(a) (b) (c) (d)

Fig. 8. CCD video camera images (a) Timing light frame showing the sample location to be observed. (b) 293 K data with electron beam on sample. (c) 40 K data with electron beam on sample. (d) 40 K data with electron beam on sample showing an arc event.

and at ~91 s elapsed time the sample current spiked to over 40 nA. Additional measurements from a digital storage oscilloscope showed that these arcs were typically less than 1 µs in duration. The image from the CCD video camera provides optical confirmation of the electrical signature and provides additional information about the spatial location of the arc. Note the currents from the central region of the sample and from the sample edge region are measured independently, as shown in Fig. 9(b).

IV. Conclusion

The ultrahigh vacuum cryostat system described here has greatly extended the low temperature capabilities (<40 K to >450 K) to conduct space environment effects tests in the laboratory environment. The brief description of electron-induced luminescence and arcing tests in Section III demonstrates the importance of temperature effects on materials used in spacecraft construction. However, this single study does not illustrate the full extent of the capabilities of the apparatus. References [4], [6] and [7] detail much more extensive studies of the low temperature cathodoluminescence and electrical characteristics of thin film optical coatings using this cryostat system. Another study using this apparatus emphasizes measurements of the magnitude, rate, and time constants (varying from µs to hr) for the electrical and optical signatures of arc events similar to the one shown in Fig. 8(d) over a wide temperature range [8]. The versatility of the sample holder design with integrated quick-connect functionality has facilitated other low temperature sample testing configurations, including those for radiation induced conductivity (RIC) [9] and dark current measurements [10]. These custom parallel-plate test fixtures allow low current measurements down to ~1-50 fA at >1000 V and determination of conductivities down to $<1\cdot10^{-21}$ $(\Omega\text{-cm})^{-1}$ [10] to $5\cdot10^{-20}$ $(\Omega\text{-cm})^{-1}$ [9]. The RIC tests lasted for days, and required maintaining stable temperature for 10's hrs to allow samples to come to electrical equilibrium [9]. The constant voltage conductivity tests measured the long term (many days) decay of dark current conductivities of spacecraft materials at low temperatures [10]. The RIC and dark current conductivity tests were performed in two different locations with the cryostat assembly mounted on different vacuum chambers than described in this paper. Finally, the cryostat and the sample holder detailed in this paper will soon be used to study the temperature dependant behavior of spacecraft materials under electron beam bombardment, including secondary electron emission in juxtaposition with a hemispherical grid retarding field analyzer [11, 12] and surface charging of dielectric materials in combination with a surface voltage probe [13, 14].

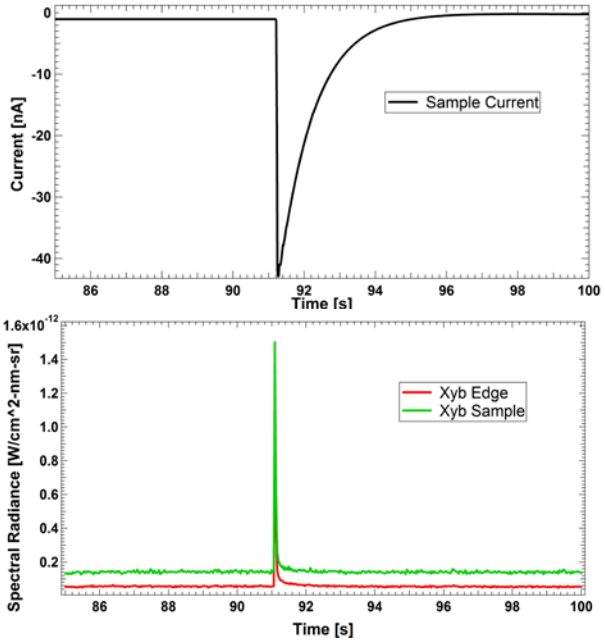

Fig. 9. Measured signatures of arcing. Electrometer current data (black). CCD Vis/NIR video camera integrated sample intensity data showing the increase in spectral radiance due to the arc event (surface glow data shown in **green**, edge glow data shown in **red**).

Acknowledgement

We gratefully acknowledge contributions to instrumentation from Tamara Jeppsen of the Materials Physics Group, Michael Taylor for the use of infrared and CCD video cameras, and useful discussions with Robert Meloy and Charles Bowers of NASA Goddard Space Flight Center. Development of the RIC and dark current measurement methods occurred during a sabbatical for Dennison sponsored by the National Research Council at the AFRL SCICL (Spacecraft Charging Instrumentation and Calibration Laboratory) and with help from Ryan Hoffmann and Dale Ferguson. This work was supported by a project for the James Webb Space Telescope Electrical Systems Group through the NASA Goddard Space Flight Center.

References

[1] W.Y. Chang, J.R. Dennison, J. Kite and R.E. Davies, "Effects of Evolving Surface Contamination on Spacecraft Charging," Paper AIAA-2000-0868, *Proc. 38th Am. Institute of Aeronautics and Astronomics Meeting on Aerospace Sci.*, (Reno, NV, 2000).

[2] JR Dennison, "The Dynamic Interplay Between Spacecraft Charging, Space Environment Interactions and Evolving Materials," *Proc. of the* 12*th Spacecraft Charging Techn. Conf.*, (Kitakyushu, Japan, May 2012).
[3] R.D Leach and M.B. Alexander, "Failures and anomalies attributed to spacecraft charging," NASA Reference Publication 1375, NASA Marshall Space Flight Center, August 1995.
[4] A. E. Jensen, G. Wilson, J. Dekany, A. M. Sim and JR Dennison "Low Temperature Cathodoluminescence of Space Observatory Materials," *Proc.* 12*th Spacecraft Charging Techn. Conf.*, (Kitakyushu, Japan, May 2012); IEEE Trans. on Plasma Sci., in press.
[5] C.D. Thomson, V. Zavyalov, and J.R. Dennison, "Instrumentation for Studies of Electron Emission and Charging from Insulators," *Proc. 8th Spacecraft Charging Techn. Conf.* (NASA Marshall Space Flight Center, Huntsville, Al, October 2003).
[6] G. Wilson, JR Dennison, A. Evans and J. Dekany "Electron Energy Dependent Charging Effects of Multilayered Dielectric Materials" *Proc.* 12*th Spacecraft Charging Techn. Conf.*, (Kitakyushu, Japan, May, 2012); IEEE Trans. on Plasma Sci., in press.
[7] JR Dennison, A. E. Jensen, G. Wilson, J. Dekany, C. W. Bowers and R. Meloy, "Electron Beam Induced Luminescence of SiO_2 Optical Coatings," Conference on Electrical Insulation and Dielectric Phenomena (CEIDP) 2012 Annual Report, IEEE-CEIDP.
[8] A. E. Jensen, JR Dennison, G. Wilson, and J. Dekany, "Nanodielectric Properties of High Conductivity Carbon-Loaded Polyimide under Electron-Beam Irradiation," *Proc. 2013 IEEE International Conf. on Solid Dielectrics (ICSD)*, (Bologna, Italy, June, 2013).
[9] R. Hoffmann, JR Dennison, A. E. Jensen, and G. Wilson, "The Correlation between Radiation Induced Conductivity (RIC) and Electron Beam Induced Luminescence in Disordered SiO_2," *Proc. 2013 IEEE International Conf. on Solid Dielectrics (ICSD)*, (Bologna, Italy, June 30-July 4, 2013).
[10] J. Dekany, A. M. Sim, J. Brunson, and JR Dennison, "Electron Transport Models and Precision Measurements in a Constant Voltage Chamber," *Proc.* 12*th Spacecraft Charging Techn. Conf.*, (Kitakyushu, Japan, May, 2012); IEEE Trans. on Plasma Sci., in press.
[11] R. Hoffmann, "Electron-Induced Electron Yields of Uncharged Insulating Materials" MS Thesis, Utah State University, Logan, UT, August 2010.
[12] RC Hoffmann and JR Dennison, "Methods to Determine Total Electron-Induced Electron Yields Over Broad Range of Conductive and Nonconductive Materials," IEEE Trans. on Plasma Sci., **40**(2), 298-304 (2012).
[13] J. Hodges, "*In Situ* Measurements of Electron Beam Induced Surface Voltage of Highly Resistive Materials," MS Thesis, Utah State University, Logan, UT, December 2012.
[14] J. L. Hodges, A. M. Sim, J. Dekany, G. Wilson, A. E. Jensen, and JR Dennison "*In Situ* Surface Voltage Measurements of Layered Dielectrics," *Proc.* 12*th Spacecraft Charging Techn. Conf.*, (Kitakyushu, Japan, May, 2012); IEEE Trans. on Plasma Sci., in press.

Justin Dekany is currently a graduate student at Utah State University in Logan, UT pursing an MS in physics. He received a BS degree in physics from USU in 2010. He has worked with the Materials Physics Group for four years on electron transport measurements, electrostatic discharge tests, electron emission measurements, and luminescence studies related to spacecraft charging. He has been the Lab Manager for the Materials Physics Group for the last two years.

Robert Johnson is a recent graduate in Mechanical Engineering from Utah State University, Logan. He has worked with the Materials Physics Group for a year and a half on thermal vacuum chamber design related to spacecraft charging, with a specialty in electron source and detector design.

Greg Wilson is currently a graduate student at Utah State University in Logan, UT pursing an MS in physics. He received BS degrees in physics and mathematics from USU in 2011. He has worked with the Materials Physics Group for two years on electron emission and luminescence studies related to spacecraft charging. He also developed a composite model for electron range over a wide range of incident energies applicable to diverse materials.

Amberly Evans is currently a graduate student at Utah State University in Logan, UT pursing an MS in physics. She received BS degrees in physics and chemistry from USU in 2012. She has worked with the Materials Physics Group for five years on electron emission, luminescence and resistivity studies and on MISSE retrieval and post-flight analysis of *SUSpECS*. Much of her work has focused on optical scattering of spacecraft materials.

J. R. Dennison received the B.S. degree in physics from Appalachian State University, Boone, NC, in 1980, and the M.S. and Ph.D. degrees in physics from Virginia Tech, Blacksburg, in 1983 and 1985, respectively. He was a Research Associate with the University of Missouri—Columbia before moving to Utah State University (USU), Logan, in 1988. He is currently a Professor of physics at USU, where he leads the Materials Physics Group. He has worked in the area of electron scattering for his entire career and has focused on the electron emission and resistivity of materials related to spacecraft charging for the last two decades.